Oxidation annealing effects on the spin-glass-like magnetism and appearance of superconductivity in T*-type $La_{1-x/2}Eu_{1-x/2}Sr_xCuO_4$ ($0.14 \leq x \leq 0.28$)

Shun Asano,[1,2,*] Kensuke M. Suzuki,[2] Kota Kudo,[1] Isao Watanabe,[3] Akihiro Koda,[4] Ryosuke Kadono,[4] Takashi Noji,[5] Yoji Koike,[5] Takanori Taniguchi,[6] Shunsaku Kitagawa,[6] Kenji Ishida,[6] and Masaki Fujita[2,4,†]

[1]*Department of Physics, Tohoku University, Aoba, Sendai 980-8578, Japan*
[2]*Institute for Materials Research, Tohoku University, Katahira, Sendai 980-8577, Japan*
[3]*Advanced Meson Science Laboratory, Nishina Center for Accelerator-Based Science, The Institute of Physical and Chemical Research (RIKEN), Wako, Saitama 351-0198, Japan*
[4]*Institute of Materials Structure Science, High Energy Accelerator Research Organization, Tsukuba, Ibaraki 305-0801, Japan*
[5]*Department of Applied Physics, Graduate School of Engineering, Tohoku University, Sendai 980-8579, Japan*
[6]*Department of Physics, Kyoto University, Kyoto 606-8502, Japan*

We investigated the magnetism and superconductivity in as-sintered (AS) and oxidation annealed (OA) T*-type $La_{1-x/2}Eu_{1-x/2}Sr_xCuO_4$ (LESCO) with $0.14 \leq x \leq 0.28$ by muon spin rotation/relaxation (μSR), magnetic susceptibility, and electrical resistivity measurements. In OA superconducting samples, no evidence of magnetic order was observed, whereas AS semiconducting samples exhibited evidence of a disordered magnetic state in the measured temperature range between ∼4 K and ∼8 K, which potentially developed toward a long-range ordered state at low temperature. Therefore, the ground state in LESCO drastically varies with oxidation annealing and the magnetic phase competitively exists with the superconducting (SC) phase. Furthermore, we clarified the simultaneous development of magnetic properties, that is, the internal magnetic field and the magnetic volume fraction, and the electrical resistivity at a low temperature in AS samples, suggesting the inducement of static magnetism by the suppression of carrier mobility. The magnetic phase in the AS LESCO is quite robust against Sr doping, while the SC phase degrades with increasing x. A monotonous decrease of the SC transition temperature from 24.5 K in $x = 0.14$ to 9.0 K in $x = 0.28$ suggests the disappearance of the SC phase at $x \sim 0.34$. These new findings for the T*-type LESCO are discussed by comparing previously reported results for T-type $La_{2-x}Sr_xCuO_4$ and T'-type $R_{2-x}Ce_xCuO_4$ (R = rare earth element) to extract common features of magnetism and their relation with superconductivity in cuprates.

I. INTRODUCTION

In the research of high superconducting-transition-temperature (T_c) superconductivity in copper oxides, the effect of the crystal structure on their physical properties is one of the fundamental issues that need to be studied in order to achieve superconductivity with higher T_c. It is well known that the optimal T_c of $La_{2-x}Sr_xCuO_4$ (∼40 K [1]) and $HgBa_2CuO_{4+\delta}$ (∼90 K [2]) systems, in both which a single CuO_2 plane is sandwiched by R_2O_2 (R = rare earth element) block layers, is quite different. A theoretical work by Sakakibara *et al* based on a two-orbital model that considers $d_{3z^2-r^2}$ in addition to $d_{x^2-y^2}$ claimed the suppression of d-wave superconductivity by a contribution of $d_{3z^2-r^2}$ to the Fermi surface [3–5]. They explained the reason for the higher T_c in $HgBa_2CuO_{4+\delta}$ through the weaker effect of $d_{3z^2-r^2}$ due to a longer distance between apical oxygen and the CuO_2 plane. Furthermore, the effect on T_c of the chemical inhomogeneity at different atomic sites in the unit cell was systematically investigated by Eisaki *et al*[6]. They clarified that chemical inhomogeneity near the apical oxygen more strongly affects the T_c than the disorder near the CuO_2 plane. These studies clearly demonstrated the importance of both global and local structural properties for the value of T_c.

Recently, the ground state of the parent R_2CuO_4 (RCO) has been discussed from a viewpoint of Cu coordination, that is, the existence/absence of apical oxygens above and below Cu ions. Naito's group first confirmed a superconducting (SC) transition in a thin film of RCO with a Nd_2CuO_4-type (T'-type) structure having CuO_4 coplanar coordination [7], which has been regarded as a Mott insulator for a long time. Superconductivity was subsequently observed by Takamatsu *et al* in low-temperature-synthesized polycrystalline samples of parent T'-type $La_{1.8}Eu_{0.2}CuO_4$[8]. From the theoretical aspect, it was shown by an ab-initio calculation conducted by Weber *et al* that the T'-type compound can have the metallic ground state, while the ground state of K_2NiF_4-type (T-type) cuprates containing CuO_6 octahedra is Mott insulating state.[9] Furthermore, Jang *et al* demonstrated the decrease of electron correlation strengths with increasing the distance between apical oxygen and the CuO_2 plane, supporting the Slater picture for T'-type [10]. Partially existing apical oxygens in the as-sintered (AS) T'-type compound are considered to prevent the appearance of superconductivity because of the introduction of random electronic potential in the CuO_2 plane [11]. Thus, a reduction annealing procedure is necessary for the complete removal of excess oxygen to

*Electronic address: shun.asano@imr.tohoku.ac.jp
†Electronic address: fujita@imr.tohoku.ac.jp

induce superconductivity in T'-type R_2CuO_4.

For a further study on the relationship between Cu coordination and the physical properties, other reference systems are important. A single-layer T*-type cuprate with CuO_5 pyramid coordination, which is formed by alternate stacks of rock-salt layers in the T-type cuprate, and by fluorite layers in the T'-type one along the c-direction, is an isomer of R_2CuO_4. Hole-doped $Nd_{2-x-y}Ce_xSr_yCuO_4$ (NCSCO) was reported as the first T*-type superconductor ($T_c \sim 32$ K). [12, 13] The AS compound shows insulating or semiconducting behavior even in the heavily hole-doped region [14], and oxidation annealing under high pressure is required for the emergence of superconductivity. The main role of annealing was reported to be the repair of oxygen vacancies [14], which is an opposite method proposed to remove apical oxygens by reduction annealing in T'-type cuprates. Therefore, studies on T*-type cuprates combined with those on T- and T'-type ones could provide vital information on the relation between Cu coordination and the physical properties, the essential role of annealing in the variation of magnetism, and the appearance of superconductivity. Many T*-type cuprates with different compositions were synthesized after the discovery of SC NCSCO [15, 16]. However, the physical properties of T*-type cuprates have been left unquestioned for a long time. This is because of the difficulties in controlling the crystal growth and in obtaining SC samples by high pressure heat treatment. Therefore, T*-type cuprates have been out of mainstream high-T_c research.

Although studies on electronic states in T*-type cuprates are quite limited, an angle-resolved photoemission spectroscopy (ARPES) measurement can clarify the electronic structure of T*-type superconductors[17]. Different features in the ARPES spectra from those for underdoped $La_{2-x}Sr_xCuO_4$ (LSCO) [18] with larger magnitude of pseudogap in $SmLa_{0.85}Sr_{0.15}CuO_4$ suggests a distinct doping evolution of the electric structure between T*- and T-type cuprates. Thus, the investigation of doping effects on the magnetic properties is important. Regarding the magnetism of T*-type cuprates, the three-dimensional magnetic order in the undoped parent $La_{1.2}Tb_{0.8}CuO_4$ was observed by muon spin rotation/relaxation (μSR) measurements in the early stage of research[19]. However, to the best of the authors' knowledge, until our recent μSR measurement on AS $La_{0.9}Eu_{0.9}Sr_{0.2}CuO_4$, no experimental study on magnetism of carrier-doped T*-type cuprates has been reported. Therefore, the magnetism in the SC phase and the doping evolution of spin correlations are still unknown.

In this paper, we revisited T*-type cuprates and elucidated the magnetic and SC properties with the aim of complementing the lack of basic knowledge for the above relevant issues. Our preliminary μSR measurement on AS $La_{1-x/2}Eu_{1-x/2}Sr_xCuO_4$ (LESCO) with $x = 0.20$ exhibited the development of magnetism at a low temperature[20]. Therefore, by extending the μSR study on LESCO, the effect of hole-doping and oxidation annealing on the inherent magnetism in T*-type cuprate can be clarified.

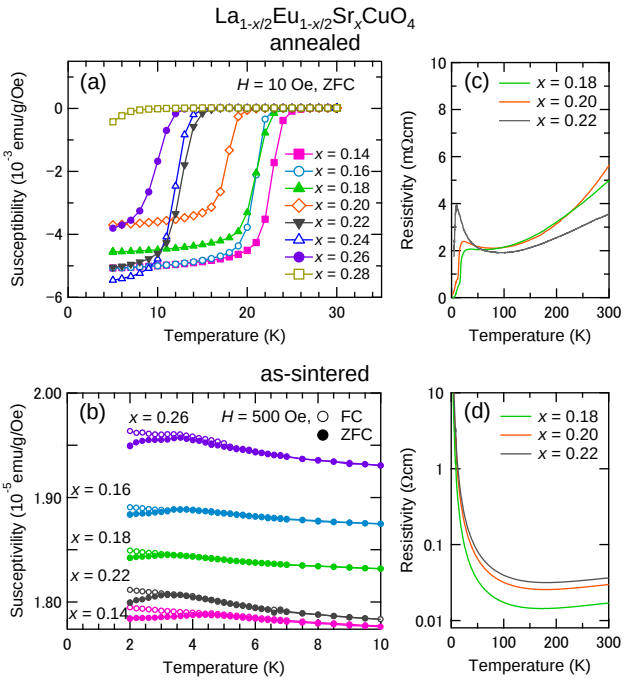

FIG. 1: (Color online) (a) Magnetic susceptibility of oxidation annealed (OA) $La_{1-x/2}Eu_{1-x/2}Sr_xCuO_4$ with $x = 0.14$–0.28 in a magnetic field of 10 Oe after zero field cooling, and (b) that of as-sintered (AS) ones measured under zero-field-cooled (closed circles) and field-cooled (open circles) processes with a field of 500 Oe. Electrical resistivity for (c) OA and (d) AS $La_{1-x/2}Eu_{1-x/2}Sr_xCuO_4$ with $x = 0.18$, 0.20, and 0.22.

II. SAMPLE PREPARATION AND EXPERIMENTAL DETAILS

The polycrystalline samples of LESCO with $0.14 \leq x \leq 0.28$ were synthesized by a solid-state reaction method. Dried powders of La_2O_3, Eu_2O_3, $SrCO_3$, and CuO were mixed with the nominal composition. The mixture was pressed into pellets and sintered at 1050 °C in air with intermediate grindings. The oxygenized samples were prepared by annealing the AS samples in oxygen gas under 40 MPa at 500 °C for 80 h. The phase purity of the samples was checked by X-ray powder diffraction measurements. Samples with $x > 0.14$ were confirmed to be single phase T*-type cuprates, while $x = 0.14$ sample contained impurity phase with a volume fraction of ~7 % of T'-type cuprate. The value of oxygen gain through annealing (y) was evaluated to be 0.023–0.024 per formula unit for $x = 0.18$, 0.20, 0.22, and 0.26 from the variation of sample weight. Although the y for other samples was not determined, we confirmed the

increase of the c-lattice constant (decrease of a-lattice constant) in all samples after annealing, suggesting an introduction of oxygens.

Magnetic susceptibility was measured for AS and OA LESCO using a superconducting quantum interference device. We furthermore performed electrical resistivity measurements for $x = 0.18$, 0.20, and 0.22 samples with a standard dc four-probe method. Zero-field (ZF) and longitudinal-field (LF) μSR measurements were carried out using a pulsed positive muon beam on the spectrometer (CHRONUS) at Port 4 in the RIKEN-RAL Muon Facility in the Rutherford Appleton Laboratory, UK, and the D1 and S1 (ARTEMIS) spectrometers in the Materials and Life Science Experimental Facility in J-PARC, Japan. In most of the measurements, the samples were cooled down to 4 K using an open-cycle ^{4}He-flow cryostat. Only the AS LESCO with $x = 0.14$ was cooled down to 1.9 K using a cryostat different from that used for measurements above 4 K. The time (t) evolution of muon spin polarization (μSR time spectra, ($A(t)$)) after the implantation of muons into the sample was measured by the asymmetry of the decay positron emission rate between forward and backward counters.

III. RESULTS

A. Magnetic susceptibility and electrical resistivity measurements

Figures 1(a) and 1(b) show the temperature dependencesof magnetic susceptibility measured in a magnetic fields of 10 Oe and 500 Oe for OA and AS LESCO with various x from 0.14 to 0.28, respectively. The Meissner effect attributed to the appearance of the SC state was observed in all the OA samples, although the signal was weak in $x = 0.28$. In contrast, in the AS samples, no evidence of SC transition was confirmed, however, spin-glass-like field dependent behavior was confirmed. As seen in Fig. 1(b), the susceptibility measured in a magnetic field of 500 Oe under zero-field-cooled (ZFC) and field-cooled (FC) processes shows different behaviors at low temperature, which is typical for a spin-glass (SG) system. We evaluated the onset temperature for the appearance of the SC state (T_c) in OA samples and the characteristic temperature at which the ZFC susceptibility in AS samples shows a local maximum (T_{sg}). T_c and T_{sg} are summarized in Fig. 6 and Fig. 7(a) as a function of x.

The temperature dependence of electrical resistivity (ρ) for OA and AS LESCO with $x = 0.18$, 0.20, and 0.22 is shown in Figs. 1(c) and 1(d). The ρ for all AS samples shows semiconducting behavior. Upon cooling, the ρ slightly decreases and rapidly increases at low temperature, indicating the existence of carriers and the strong localization of carriers. In the OA samples, the ρ is lower in the entire temperature range and exhibits metallic behavior above ∼100 K. However, ρ shows an upturn and increases upon cooling, followed by a rapid drop associated with the emergence of superconductivity. Therefore, the oxygenation annealing enhances the metallicity but the chemical disorder would slightly remain in the OA samples, which causes impurity scattering.

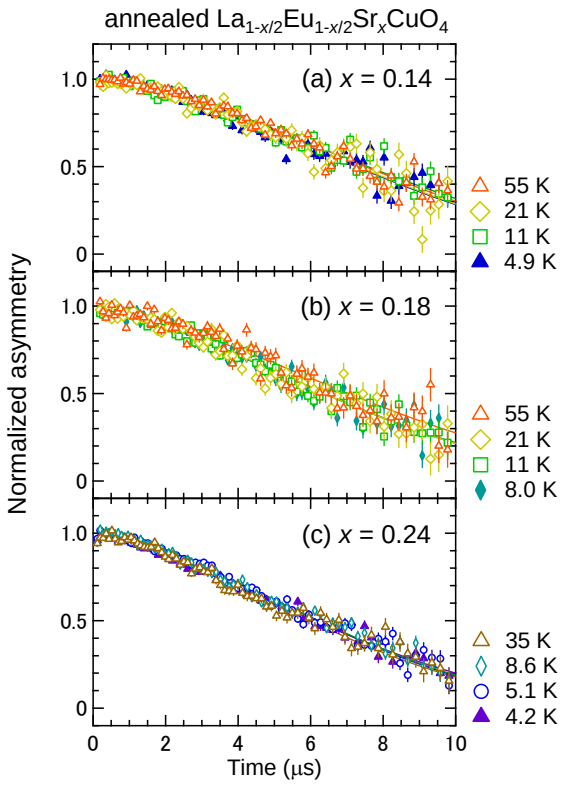

FIG. 2: (Color online) Zero-field μSR time spectra of oxidation annealed $La_{1-x/2}Eu_{1-x/2}Sr_xCuO_4$ with (a) $x = 0.14$, (b) 0.18, and (c) 0.24. The solid curves are fitted results using the first term of Eq. (1).

B. Zero-field μSR measurements

We first investigated the Cu spin dynamics in OA LESCO by ZF-μSR measurements. Figure 2 shows normalized μSR time spectra for OA LESCO with $x = 0.14$, 0.18, and 0.24. All spectra show Gaussian-type depolarization above 4 K and the thermal evolution of the spectra is negligible. This Gaussian-type depolarization is originated from the nuclear-dipole field, indicating neither static nor dynamic fluctuating Cu spins within the μSR time window. Absence of magnetic order in the present LESCO is consistent with the results for $La_{2-x}Sr_xCuO_4$ ($x = 0.15$–0.20)[21], $Bi_2Sr_{2-x}La_xCuO_{6+\delta}$ (hole concentration, $p\sim$ 0.15–0.20) [22], and $Bi_{1.76}Pb_{0.35}Sr_{1.89}CuO_{6+\delta}$ ($p > 0.09$) [23], and therefore, is a common feature of optimally-doped and overdoped (OD) single layer cuprate superconductors.

In contrast to the absence of static magnetism in the

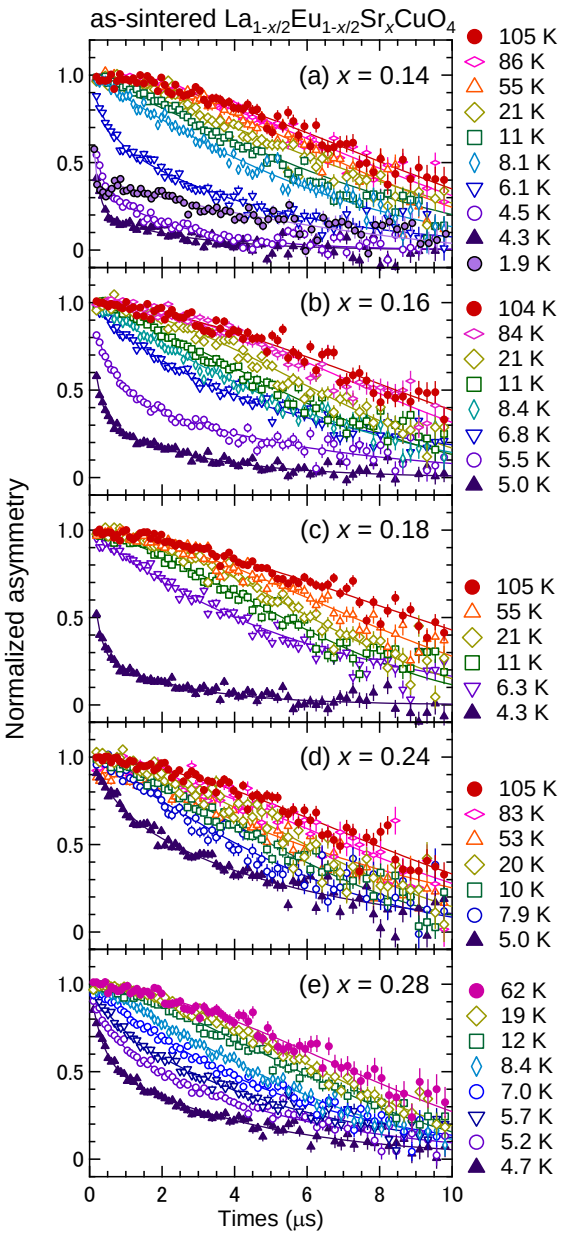

FIG. 3: (Color online) Zero-field μSR time spectra of as-sintered $La_{1-x/2}Eu_{1-x/2}Sr_xCuO_4$ with (a) $x = 0.14$, (b) 0.16, (c) 0.18, (d) 0.24, and (e) 0.28. The solid curves are fitted results using Eq. (1) for the data collected above 4 K.

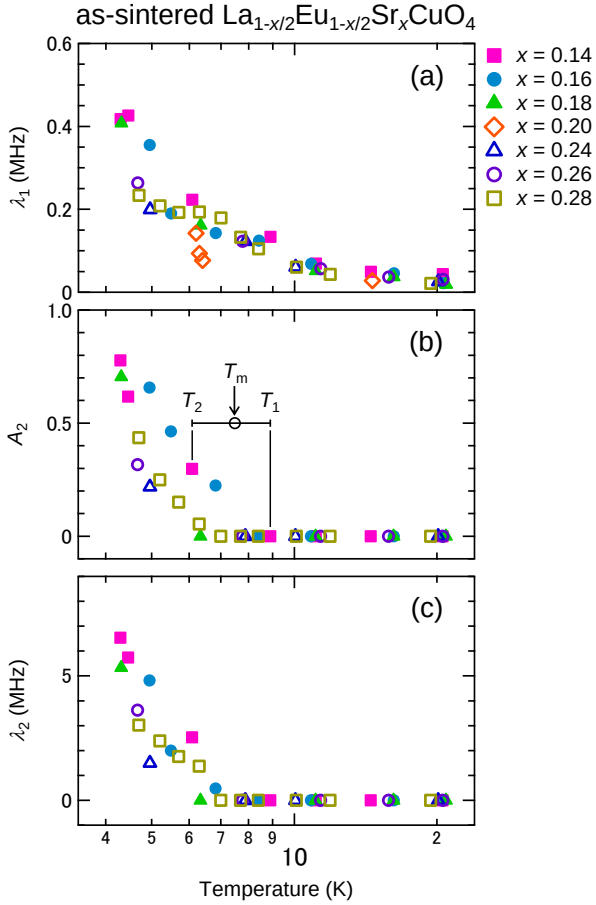

FIG. 4: (Color online) Temperature dependence of (a) muon-spin depolarization rate λ_1 of the slow depolarizing component, (b) initial asymmetry A_2 and (c) depolarization rate λ_2 of the fast depolarizing component in Eq. (1) for as-sintered $La_{1-x/2}Eu_{1-x/2}Sr_xCuO_4$ ($0.14 \leq x \leq 0.28$). T_m is the intermediate point between the lowest temperature where $A_2 = 0$ (T_1) and the first temperature where A_2 has a finite value upon cooling (T_2).

OA samples, an appearance of (quasi) static magnetism was confirmed in AS non-SC LESCO samples with $0.14 \leq x \leq 0.28$. Figure 3(a) shows ZF-μSR time spectra in AS LESCO with $x = 0.14$. The spectrum at 105 K shows Gaussian-type depolarization due to the nuclear-dipole field, as observed in OA LESCO. Upon cooling, the Gaussian-type depolarization changes into an exponential-type one, indicating the development of Cu spin correlations. At 1.9 K, the spectrum shows oscillating behavior, indicating the existence of coherent magnetic order. Therefore, the magnetic properties evolve toward the long-range order with decreasing the temperature. The spectral change from Gaussian-type depolarization to exponential-type one was observed in all AS LESCO with $0.16 \leq x \leq 0.28$, including previously reported $x = 0.20$[20]. Thus, the magnetism would develop toward the long-range order occurred in a wide x range of $0.14 \leq x \leq 0.28$ in AS LESCO. Comparing the spectra at low temperature of 4–5 K for all samples shown in Fig. 3, the depolarization seems slightly slower with increasing x, suggesting a weak degradation of magnetism upon doping.

For the quantitative analysis of the μSR time spectra in AS LESCO above 4 K, we fitted the following function to the obtained data.

$$A(t) = A_1 e^{-\lambda_1 t} G(\Delta, t) + A_2 e^{-\lambda_2 t}, \qquad (1)$$

where $A_1 + A_2 = 1$. The first (second) term represents the slow (fast) depolarizing component due to fast (slow) Cu fluctuations. $G(\Delta, t)$ is the static Kubo–Toyabe function and Δ is the half-width of the nuclear dipole field distributed at the muon site. A_1 (A_2) and λ_1 (λ_2) are initial asymmetry and depolarization rates of the slow (fast) depolarizing component, respectively. The spectra above 4 K are well reproduced by Eq. (1) for all samples, as shown by solid curves in Fig. 3. In the fitting analysis for the spectrum at 1.9 K of the $x = 0.14$ sample, we added a rotation component, $e^{-\lambda_3 t}\cos(2\pi f t + \phi)$, to Eq. (1), where λ_3, f, and ϕ are damping rate, frequency, and phase of the muon spin precession.

Figure 4(a) presents the evaluated λ_1 as a function of temperature. As seen in the figure, λ_1 grows at low temperature upon cooling in all AS samples. Although λ_1 for all samples starts to increase at almost the same temperature of ∼20 K, the value of λ_1 at 4–5 K appears larger in the sample with smaller x; λ_1 of ~ 0.4 for $0.14 \leq x \leq 0.18$ and ~ 0.2 for $0.24 \leq x \leq 0.28$. Similarly, A_2 and λ_2 for all the measured samples increase with decreasing the temperature. (See Figs. 4(b) and 4(c).) This means that the short-range magnetically ordered state and/or a dynamically fluctuating spin state within the μSR time window took place in the sample. A_2 at the lowest temperatures measured (4–5 K) was 0.3-0.8 and tended to increase with further cooling, suggesting that the magnetic ground state in the present AS samples is of bulk. The values of A_2 and λ_2 at 4–5 K slightly decreased with increasing x, similar to the trend of the x-dependence of λ_1. To evaluate the temperature for the appearance of the fast component in the time spectra, we defined $T_{\rm m}$ as the intermediate point between the lowest temperature where $A_2 = 0$ (T_1) and the first temperature where A_2 has a finite value upon cooling (T_2). (See Fig. 4(b).) Although the measured temperature points are not too many, the $T_{\rm m}$ for a wide x range shows a weak x-dependence. In Fig. 7(a), $T_{\rm m}$ is plotted together with $T_{\rm sg}$, exhibiting the magnetic phase diagram for AS LESCO.

Using the Kubo–Toyabe function in Eq. (1), we analyzed the spectra of SC LESCO shown in Fig. 2. The fitted results yielded an almost constant value of $\lambda_1 \sim$ of 0.01 MHz for all samples in the temperature range between 4–60 K.

C. Longitudinal-field μSR measurements

The magnetic state of AS LESCO at low temperatures was further investigated by LF-μSR measurements. Figure 5(a) shows the field dependence of LF-μSR time spectra for the $x = 0.14$ sample at 4.3 K. Below 1000 Gauss, the depolarization of the spectra at longer time ranges was upwardly shifted with applying the magnetic field, whereas the field effect on the spectra in the vicinity of $t = 0$ showing the rapid depolarization was negligible. With further increasing the field above 2000 Gauss, the overall spectra from $t = 0$ were shifted; therefore, a static magnetic field lower than ∼2000 Gauss was present at the muon stopping site. The successive shift of the overall spectrum with the application of fields above 2000 Gauss suggests the existence of a fast fluctuating local field as well. Therefore, this sequential field dependence indicates the coexistence of static magnetic ordered and dynamically fluctuating spin states in the $x = 0.14$ sample at 4.3 K. Similar field dependence of the LF-μSR time spectra was observed for the $x = 0.18$ sample at 4.95 K, as seen in Fig. 5(b), suggesting that the appearance of disordered magnetic state is common for the AS LESCO with a wide x range.

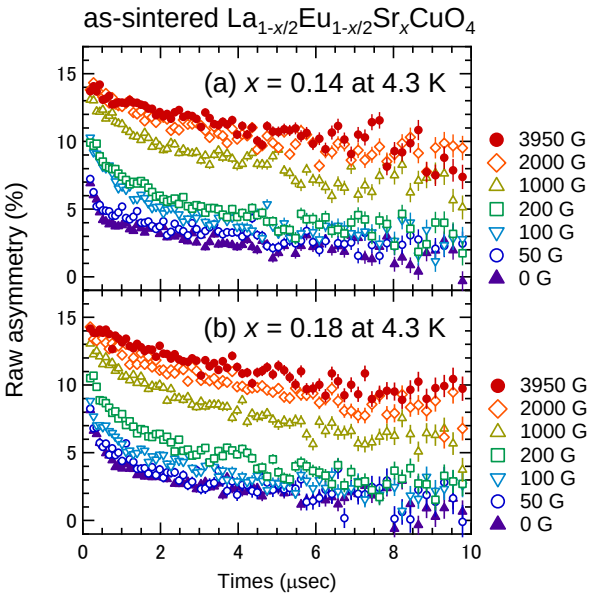

FIG. 5: (Color online) Longitudinal-field μSR time spectra in as-sintered $La_{1-x/2}Eu_{1-x/2}Sr_xCuO_4$ with (a) $x = 0.14$ at 4.3 K and with (b) 0.18 at 4.3 K.

IV. DISCUSSION

A. Magnetic and superconducting phase diagram

Figure 6 and 7 (a) summarize $T_{\rm c}$ for the OA LESCO, and $T_{\rm m}$ and $T_{\rm sg}$ for AS LESCO. $T_{\rm c}$ for T*-type $SmLa_{1-x}Sr_xCuO_4$ (SLSCO) is also plotted as a reference [24]. In the present study, the $x = 0.14$ sample showed the maximum $T_{\rm c}$ and $T_{\rm c}$ decreased monotonically with increasing x, indicating that the present samples are located in the OD region. An extrapolation of the x-dependence of $T_{\rm c}$ yields $T_{\rm c} = 0$ at $x \sim 0.34$ ($x_{\rm c}$), which is comparable to the critical value for the disappearance of the SC phase in T-type LSCO [25]. On the contrary, almost a constant $T_{\rm m}$ and $T_{\rm sg}$ against x in the present AS LESCO implies the existence of magnetism far beyond $x_{\rm c}$. Consistently, the critical x value for $A_2 = 0$

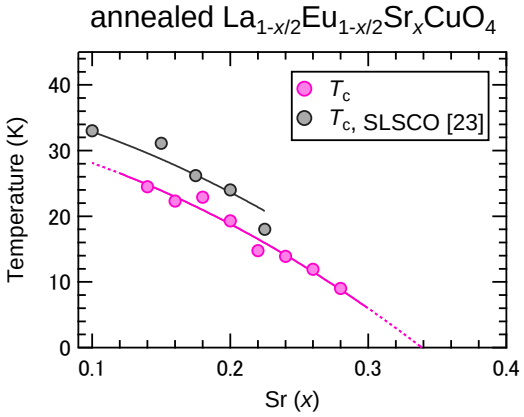

FIG. 6: (Color online) Sr concentration dependences of T_c in the oxidation annealed $La_{1-x/2}Eu_{1-x/2}Sr_xCuO_4$ and one. Solid lines are guides to the eyes. T_c for $SmLa_{1-x}Sr_xCuO_4$ (SLSCO) was taken from Ref.[24] is also plotted for reference.

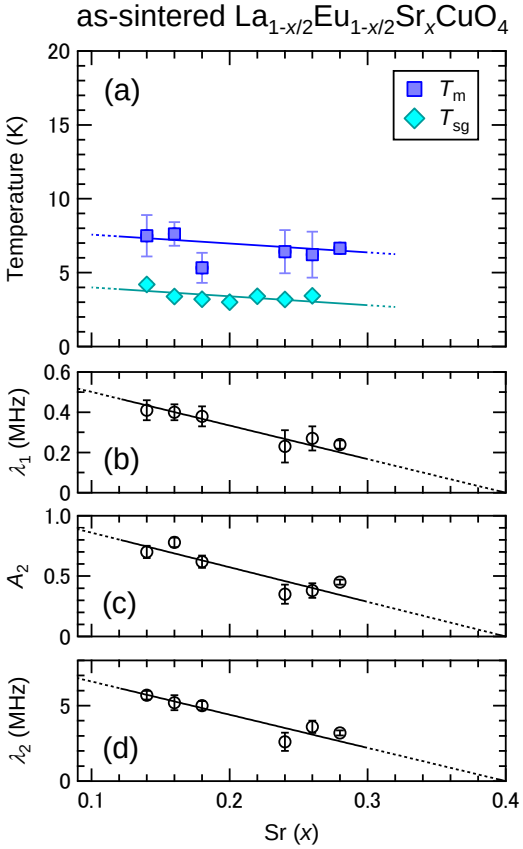

FIG. 7: (Color online) (a) Sr concentration dependences of T_m and T_{sg} for as-sintered $La_{1-x/2}Eu_{1-x/2}Sr_xCuO_4$. Solid lines are guides to the eyes. Sr concentration dependence of (b) λ_1, (c) A_2, and (d) λ_2 at 4.5 K.

and $\lambda_2 = 0$ is estimated to be $\sim$0.4 from the extrapolation of x-dependence of A_2 and λ_2 at 4.5 K. (See Fig. 7(c)–7(d).) Note that for each sample we evaluated λ_1, A_2 and λ_2 at 4.5 K from the interpolation or extrapolation of temperature dependence of values shown in Fig. 4(b)–4(d).

In the parent compound of T*-type $La_{1.2}Tb_{0.8}CuO_4$, the magnetic order takes place below $\sim$280 K [19]. Given the onset temperature of 280 K for the appearance of static magnetism in the T*-type parent compound, which is comparable with Néel temperature in T-type La_2CuO_4 [26] and T'-type R_2CuO_4 [27], the present results showing disordered (no) magnetic order in AS (OA) T*-type LESCO suggest the full suppression of long-range magnetic order at $x < 0.14$. This trend was similar to the drastic suppression of Néel order by hole-doping in LSCO. [26] Therefore, the magnetic and superconducting phase diagrams in the hole-doped T*- and T-type cuprates are quantitatively the same, while the electronic structure in two systems is different [17, 18, 29].

B. Origin of variation in magnetism due to oxidation annealing

Here, we discuss the origin of the variation in magnetism due to oxidation annealing in T*-type LESCO. First, the electrical resistivity measurements exhibit the semiconducting nature of AS samples, and therefore, the magnetism at low temperature corresponds to the localized Cu spins. Formation of the magnetic state is likely mediated by super-exchange couplings among the Cu spins, but not induced by Ruderman–Kittel–Kasuya–Yosida interaction, which is proposed to understand the magnetism in OD $La_{2-x}Sr_xCu_{1-y}Fe_yO_4$ [33–35]. Within the localized spin picture, following are the possible origins of disappearance of magnetic order due to oxidation annealing;

1) Increase of hole concentration,
2) Removal of chemical disorder.

In case 1, spin correlations degrade owing to the increase in the hole concentration. Oxidation of the sample causes the increase in the hole concentration due to the charge neutrality, and the carrier doping weakens the static spin correlations. Therefore, superconductivity could emerge with degradation of spin correlations caused by the doping of a sufficient number of holes. The increased number of oxygens by the annealing (y) is $\sim$0.024 per formula unit for the present samples, suggesting that the additionally doped holes at a fixed Sr concentration is 5% at most. However, even though the Sr concentration, which corresponds to hole concentration, increases by 5% in the AS LESCO, the system remains magnetic state and does not show superconductivity. Therefore, hole-doping by oxidation annealing is not the direct origin of the disappearance of magnetism.

Regarding case 2, the enhancement of spin fluctuations could be attributed to the removal of chemical disorders. Considering the experimental fact that the magnetic properties concomitantly develop with the rapid

increase of resistivity below a comparable temperature (∼5–10 K), the suppression of carrier mobility induces the static magnetism. The suppression of mobility in the AS sample hence originate from the localization of the carrier by the chemical defects.

There are three possible oxygen sites, which induces random potential on the CuO_2 plane: (i) apical oxygen site, (ii) oxygen site in the CuO_2 plane and (iii) interstitial oxygen site. The elongation of c-lattice constant after oxidation annealing suggests the insertion of oxygen between the CuO_2 planes, supporting the case (i) and (iii). It was indicated that the effect of local disorder on T_c was more marked in T*-type cuprates than in other single-layer ones, because of the shorter distance between Cu and apical oxygens [24]. By the same reason, the disorder due to apical oxygen in T*-type cuprates could more markedly affect the spin and electric correlations on the CuO_2 planes. The effect of disorder at the interstitial oxygen sites, which are away from the CuO_2 plane, could be negligible. Thus, the main reason for the variation in magnetism due to oxidation annealing is most likely related to the apical oxygen.

C. Relevance to T-type $La_{2-x}Sr_xCuO_4$

We further discuss the magnetism in AS T*-type LESCO in comparison with that in T-type LSCO. As mentioned above, AS LESCO exhibits semiconducting behavior and the magnetism is similar to that in the lightly hole doped SG phase of other single-layer systems. T_{sg} in AS LESCO is comparable to that in LSCO (T_{sg} = 5–6 K) [37] and in $Bi_{2+x}Sr_{2-x}CuO_{6+\delta}$ (T_{sg} = 3–4 K) [38, 39]. Therefore, the appearance of SG phase after the suppression of long-range magnetic order by hole-doping is common for the single-layer cuprate. However, the SG region in LESCO is quite broad against Sr concentration. In AS LESCO, doped holes would be localized in the CuO_2 plane near the defects, and therefore, the number of effective mobile carriers as well as the mobility are considered to be lower than those in LSCO with the comparable x. The larger localization of hole carriers due to disorder in apical oxygen site possibly result into the insensitive x-dependence of T_{sg} and T_m in AS LESCO.

Assuming that the present AS LESCO corresponds to the SG phase of LSCO, the oxidation annealing dramatically changes the electronic state, that is, the ground state of LESCO varies from SG to OD region through annealing. It is worth mentioning that, in the SG (SC) phase of LSCO and $Bi_{2+x}Sr_{2-x}CuO_{6+\delta}$, the spin-density-wave with the modulation diagonal (parallel) to the Cu-O bonding direction in the CuO_2 plane can be observed by neutron scattering measurements [39, 40]. The direction and the period of modulation change upon doping. Therefore, observation of spatial spin correlations as well as evaluation of actual carrier number in both AS and OA samples provide crucial information for understanding the origin of magnetism in T*-type LESCO.

D. Relevance to T'-type $R_{2-x}Ce_xCuO_4$

The existence of weak magnetism in the AS sample and the suppression due to annealing were recently reported for T'-type R_2CuO_4, and the origin was discussed in connection with structural defects [41]. In the AS sample of T'-type R_2CuO_4, at high temperatures between 150 K and 280 K, a partially ordered spin state with a volume fraction of 20-30% coexists with the underlying inhomogeneous spin state. This partially ordered state disappears by oxygen reduction annealing, while the inhomogeneous spin state remains in the annealed samples. Therefore, the weak magnetism in the AS T*-LESCO and AS T'-type R_2CuO_4 is relatively different. Furthermore, in the T'-type R_2CuO_4, the three-dimensional magnetic order was achieved in both the AS and the reduction annealed samples below ∼120 K, and no annealing effect on the ordering temperature (T_{N2}) was reported [41]. These results, combined with the structural study on the T'-type cuprates [42], suggest that the chemical disorder in the T'-type cuprates locally affects the magnetic fluctuation and/or the short-range magnetic order, resulting in the inducement and/or enhancement of partial static magnetism. In other words, spin fluctuations are directly suppressed by the disorders around them, which is contrastive to the slowing down of fluctuations in the entire sample through carrier localization. Therefore, the enhancement of (quasi) static magnetism would be caused in a different manner by the excess oxygen in T'-type RCO and by the oxygen defect in T*-type LESCO.

In contrast to the obvious annealing effect on weak magnetism, the absence of long range order in the AS T*-type LESCO and no change of T_{N2} by annealing in the T'-type RCO imply that Néel order is hardly formed by chemical disorders in both systems. This suggests that the drastic suppression of AF ordered states due to annealing in the T'-type $R_{2-x}Ce_xCuO_4$ with larger x [27, 28, 43] is not directly caused by the removal of disorder. Recent ARPES [44, 45] and Cu K-edge X-ray absorption near-edge structure measurements [46] clarified aspects of electron doping in the annealing effect. Thus, the degradation of the AF order due to annealing in T'-type RCO would be predominantly caused by electron doping. These results furthermore yield a clue for understanding the undoped superconductivity in T'-type R_2CuO_4. Following the above discussion, if the disorder is introduced in SC R_2CuO_4, a weak magnetism is expected to emerge, but Néel order would not be induced. Indeed, thin films and low-temperature-synthesized AS T'-type R_2CuO_4, which are reported to show superconductivity after annealing, have rather low T_m [47]. Thus, the clarification of individual magnetism in the AS material of Ce-free superconductors and the conventionally synthesized R_2CuO_4 are important ways to understand the material dependent physical properties.

V. SUMMARY

We performed the first systematic μSR study of magnetism in T*-type cuprates using $La_{1-x/2}Eu_{1-x/2}Sr_xCuO_4$ with $0.14 \leq x \leq 0.28$. It was found that all AS semiconducting samples exhibit SG-like magnetism below $\sim$8 K. The size of Cu spin moment and the magnetic volume fraction concomitantly grow with the increase of electrical resistivity upon cooling, indicating a close relation between the magnetism and the mobility of carriers. The magnetic phase is robust against x but fully suppressed in the OA samples, suggesting the competitive relation between disordered magnetic and SC states. This significant variation in the ground state of T*-type $La_{1-x/2}Eu_{1-x/2}Sr_xCuO_4$ by oxidation annealing yields a unique opportunity for the study of the interplay between spin correlations and superconductivity, which strongly depends on the hole concentration.

Acknowledgments

The μSR experiments at the RIKEN-RAL Muon Facility in the Rutherford Appleton Laboratory (Proposal No.RB1670580) and at the Materials and Life Science Experimental Facility of J-PARC (Proposal Nos. 2015MP001 and 2018B0324) were performed under user programs. We greatly thank the RIKEN-RAL and the J-PARC staff for their technical support during the experiments, and Y. Ishikawa for his contribution in administrative work for IMSS. We also acknowledge helpful discussions with T. Adachi, K. M. Kojima, and Y. Miyazaki. This work was supported by MEXT KAKENHI, Grant Numbers 16H02125, the IMSS Multiprobe Research Grant Program, and IMSS Quantum Beam Research Grant.

[1] H. Takagi, T. Ido, S. Ishibashi, M. Uota, S. Uchida and Y. Tokura, Phys. Rev. B **40**, 2254 (1989).

[2] A. Yamamoto, W.-Z. Hu, and S. Tajima, Phys. Rev. B **63**, 024504 (2000).

[3] H. Sakakibara, H. Usui, K. Kuroki, R. Arita, and H. Aoki, Phys. Rev. Lett. **105**, 057003 (2010).

[4] H. Sakakibara, H. Usui, K. Kuroki, R. Arita, and H. Aoki, Phys. Rev. B **85**, 064501 (2012).

[5] H. Sakakibara, K. Suzuki, H. Usui, K. Kuroki, R. Arita, D. J. Scalapino, and H. Aoki, Phys. Rev. B **86**, 134520 (2012).

[6] H. Eisaki, N. Kaneko, D. L. Feng, A. Damascelli, P. K. Mang, K. M. Shen, Z.-X. Shen, and M. Greven, Phys. Rev. B **69**, 064512 (2004).

[7] A. Tsukada, Y. Krockenberger, M. Noda, H. Yamamoto, D. Manske, L. Alff, and M. Naito, Solid State Commun. **133**, 427 (2005).

[8] T. Takamatsu, M. Kato, T. Noji, and Y. Koike, Appl. Phys. Express **5**, 073101 (2012).

[9] C. Weber, K. Haule, and G. Kotliar, Phys. Rev. B **82**, 125107 (2010).

[10] S. W. Jang, H. Sakakibara, H. Kino, T. Kotani, K. Kuroki, and M. J. Han, Sci. Rep. **6**, 33397 (2016).

[11] T. Adachi, T. Kawamata, and Y. Koike, Condens. Matter **2**, 23 (2017).

[12] J. Akimitsu, S. Suzuki, M. Watanabe, and H. Sawa, Jpn. J. Appl. Phys. **27**, L1859 (1989).

[13] H. Sawa, S. Suzuki, M. Watanabe, J. Akimitsu, H. Matsubara, H. Watabe, S. Uchida, K. Kokusho, H. Asano, F. Izumi, and E. Takayama-Muromachi, Nature **337**, 347 (1989).

[14] F. Izumi, E. Takayama-Muromachi, A. Fujimori, T. Kamiyama, H. Asano, J. Akimitsu, and H. Sawa, Physica C **158**, 440 (1989).

[15] S-W. Cheong, Z. Fisk, J. D. Thompson, and R. B. Schwarz, Physica C **159**, 407 (1989).

[16] Z. Fisk, S-W. Cheong, J. D. Thompson, M. F. Hundley, R. B. Schwarz, G. H. Kwei, and J. E. Schirber, Physica C **162**, 1681 (1989).

[17] A. Ino, M. Higashiguchi, K. Yamazaki, T. Yamasaki, T. Narimura, K. Kobayashi, K. Shimada, H. Namatame, M. Taniguchi, T. Yoshida, A. Fujimori, Z.-X. Shen, T. Kakeshita, S. Uchida, S. Adachi, and S. Tajima, Physica B, **351**, 274 (2004).

[18] A. Lanzara, P. V. Bogdanov, X. J. Zhou, S. A. Kellar, D. L. Feng, E. D. Lu, T. Yoshida, H. Eisaki, A. Fujimori, K. Kishio, J.-I. Shimoyama, T. Noda, S. Uchida, Z. Hussain, and Z.-X. Shen, Nature **412**, 510 (2001).

[19] A. Lappas and K. Prassides, A. Amato, R. Feyerherm, F.N. Gygax, and A. Schenck, Hyperfine Interactions **86**, 555 (1994).

[20] M. Fujita, K. M. Suzuki, S. Asano, A. Koda, H. Okabe, and R. Kadono, JPS Conf. Proc. **21**, 011026 (2018).

[21] T. Adachi, N. Oki, Risdiana, S. Yairi, Y. Koike, and I. Watanabe, Phys. Rev. B **78**, 134515 (2008).

[22] P. L. Russo, C. R. Wiebe, Y. J. Uemura, A. T. Savici, G. J. MacDougall, J. Rodriguez, G. M. Luke, N. Kaneko, H. Eisaki, M. Greven, O. P. Vajk, S. Ono, Y. Ando, K. Fujita, K. M. Kojima, and S. Uchida, Phys. Rev. B **75**, 054511 (2007).

[23] M. Miyazaki, R. Kadono, M. Hiraishi, K. H. Satoh, S. Takeshita, A. Koda, Y. Fukunaga, Y. Tanabe, T. Adachi, and Y. Koike, Physica C **470**, s55 (2010)

[24] T. Kakeshita, S. Adachi, and S. Uchida, J. Phys. Conf. Ser. **150**, 052089 (2009).

[25] Y. Tanabe, T. Adachi, T. Noji, and Y. Koike, J. Phys. Soc. Jpn. **74**, 2893 (2005).

[26] B. Keimer, N. Belk, R. J. Birgeneau, A. Cassanho, C. Y. Chen, M. Greven, M. A. Kastner, A. Aharony, Y. Endoh, R. W. Erwin, and G. Shirane, Phys. Rev. B **46**, 14034 (1992).

[27] G. M. Luke, L. P. Le, B. J. Sternlieb, Y. J. Uemura, J. H. Brewer, R. Kadono, R. F. Kiefl, S. R. Kreitzman, T. M. Riseman, C. E. Stronach, M. R. Davis, S. Uchida, H. Takagi, Y. Tokura, Y. Hidaka, T. Murakami, J. Gopalakrishnan, A. W. Sleight, M. A. Subramanian, E. A. Early,

J. T. Markert, M. B. Maple, and C. L. Seaman, Phys. Rev. B **42**, 7981 (1990).
[28] T. Uefuji, T. Kubo, K. Yamada, M. Fujita, K. Kurahashi, I. Watanabe, and K. Nagamine, Physica C **357**, 208 (2001).
[29] T. Yoshida, X. J. Zhou, K. Tanaka, W. L. Yang, Z. Hussain, Z.-X. Shen, A. Fujimori, S. Sahrakorpi, M. Lindroos, R. S. Markiewicz, A. Bansil, Seiki Komiya, Yoichi Ando, H. Eisaki, T. Kakeshita, and S. Uchida, Phys. Rev. B **74**, 224510 (2006).
[30] A. R. Moodenbaugh, Y. Xu, M. Suenaga, T. J. Folkerts and R. N. Shelton, Phys. Rev. B **38**, 4596 (1988).
[31] M. K. Crawford, R. L. Harlow, E. M. McCarron, W. E. Farneth, J. D. Axe, H. Chou, and Q. Huang, Phys. Rev. B **44**, 7749 (1991).
[32] M. Ambai, Y. Kobayashi, S. Iikubo, and M. Sato, J. Phys. Soc. Jpn. **71**, 538 (2002).
[33] M. Fujita, M. Enoki, and K. Yamada, J. Phys. Chem. Solids **69**, 3167 (2008).
[34] R.-H. He, M. Fujita, M. Enoki, M. Hashimoto, S. Iikubo, S.-K. Mo, H. Yao, T. Adachi, Y. Koike, Z. Hussain, Z.-X. Shen, and K. Yamada, Phys. Rev. Lett. **107**, 127002 (2011).
[35] K. M. Suzuki, T. Adachi, H. Sato, I. Watanabe, and Y. Koike, J. Phys. Soc. Jpn. **85**, 124705 (2016).
[36] Y. Ueda, Y. Fujiwara, A. Hayashi, K. Shibutani, and R. K. Ogawa, Physica C **198**, 237 (1992).
[37] S. Wakimoto, S. Ueki, Y. Endoh, and K. Yamada, Phys. Rev. B **62**, 3547 (2000).
[38] M. Enoki, M. Fujita, S. Iikubo, J. M. Tranquada, and K. Yamada, J. Phys. Soc. Jpn. **80**, SB026 (2011).
[39] M. Enoki, M. Fujita, T. Nishizaki, S. Iikubo, D. K. Singh, S. Chang, J. M. Tranquada, and K. Yamada, Phys. Rev. Lett. **110**, 017004 (2013).
[40] M. Fujita, K. Yamada, H. Hiraka, P. M. Gehring, S. H. Lee, S. Wakimoto, and G. Shirane, Phys. Rev. B **65**, 064505 (2002).
[41] K. M. Suzuki, S. Asano, H. Okabe, A. Koda, R. Kadono, I. Watanabe, and M. Fujita, arXiv:1901.11233.
[42] P. G. Radaelli, J. D. Jorgensen, A. J. Schultz, J. L. Peng, and R. L. Greene, Phys. Rev. B **49**, 15322 (1994).
[43] M. Fujita, T. Kubo, S. Kuroshima, T. Uefuji, K. Kawashima, K. Yamada, I. Watanabe, and K. Nagamine, Phys. Rev. B **67**, 014514 (2003).
[44] D. Song, G. Han, W. Kyung, J. Seo, S. Cho, B. S. Kim, M, Arita, K. Shimada, H. Namatame, M. Taniguchi, Y. Yoshida, H. Eisaki, S. R. Park, and C. Kim, Phys. Rev. Lett. **118**, 137001 (2017).
[45] M. Horio, Y. Krockenberger, K. Koshiishi, S. Nakata, K. Hagiwara, M. Kobayashi, K. Horiba, H. Kumigashira, H. Irie, H. Yamamoto, and A. Fujimori, Phys. Rev. B **98**, 020505(R) (2018).
[46] S. Asano, K. Ishii, D. Matsumura, T. Tsuji, T. Ina, K. M. Suzuki, and M. Fujita, J. Phys. Soc. Jpn. **87**, 094710 (2018).
[47] T. Adachi, A. Takahashi, K. M. Suzuki, M. A. Baqiya, T. Konno, T. Takamatsu, M. Kato, I. Watanabe, A. Koda, M. Miyazaki, R. Kadono, and Y. Koike, J. Phys. Soc. Jpn. **85**, 114716 (2016).